Eur. Phys. J. B **31**, 47–52 (2003)
DOI: 10.1140/epjb/e2003-00007-9

THE EUROPEAN PHYSICAL JOURNAL B

Doping dependence of infrared conductivity of camphor-sulphonic-acid-doped polyaniline

F. Gervais[1,a], N. Petit[1], C. Popon[1], and P. Buvat[2]

[1] Laboratoire d'Électrodynamique des Matériaux Avancés[b], Université François Rabelais, Parc de Grandmont, 37200 Tours France
[2] CEA/Le Ripault, Département Matériaux, BP 16, 37260 Monts, France

Received 6 February 2002 / Received in final form 12 August 2002
Published online 27 January 2003 –

Abstract. The reflectivity spectrum of a polyaniline CSA-doped in presence of m-cresol has been measured over the wide wavenumber range 25–15,000 cm^{-1} (0.003–1.9 eV) for three different doping levels. Since spectra cannot be fitted correctly with the conventional Drude model, several extensions are tested. A model derived from the factorized form of the dielectric response and including the effect of Anderson localization in disordered metals, is proposed and found to yield good fit to data with a satisfactory physical meaning. Data are reduced to a small number of parameters potentially useful for further comparison with other conducting polymers or even other non-Drude conducting media like oxides.

PACS. 78.30.Jw Organic compounds, polymers – 72.80.Le Polymers; organic compounds (including organic semiconductors) – 71.38.+i Polarons and electron-phonon interactions

1 Introduction

Conducting polymers have attracted considerable interest since the discovery of conductivity in doped polyacetylene in 1977 [1]. They do not show, however, the basic optical properties of common metals in that (i) mirror-like reflectivity is not observed in the visible part of the electromagnetic radiation, (ii) optical conductivity is not maximum at zero frequency as in metals where it is commonly described *via* the Drude model. Conducting and superconducting oxides essentially share with conducting polymers these "non-Drude" optical properties. Among them, high-T_c cuprate superconductors are under severe debate since their discovery by Bednorz and Müller in 1986. An enormous amount of effort has gone toward the understanding of the electronic and transport properties in conducting polymers since 1977 and in conducting oxides since 1986. In both classes of materials, the same central question may be addressed: do the charge carriers form a homogeneous state that may be treated as an electron gas or a Fermi liquid as in metals, or do they form a heterogeneous state? In conducting polymers, while certain studies suggest that the conductivity is well described by the Anderson model [2] of disordered metal with homogeneous disorder occurring on length scales equal to or less than the electronic correlation length [3,4], other authors [5–7] claim the presence of a heterogeneous state in which metallic islands are embedded in an insulating matrix, the relevant disorder length scale being large compared to the electronic correlation length. Two key arguments are exploited to arrive at the conclusions. (i) The temperature dependence of the DC conductivity discriminates a thermally-assisted behavior from a more "metallic" one. (ii) The frequency dependence of both dielectric response and optical conductivity down to the far-infrared allows one to check whether the system displays a Drude-like behavior or conversely shows opposite trends. In many conducting polymer samples, the optical conductivity shows a decrease upon decreasing frequency in the far- infrared, which was early interpreted in terms of "pseudo-gap" [8,9], instead of the maximum of conductivity at zero frequency predicted by the Drude model. In addition, and contrary to conventional metals where it becomes negative below the screened plasma frequency, the real part of the dielectric response of conducting polymers remains positive in the whole spectral range. Exceptions to this common behavior in polymers have been put forward however to support the model of inhomogeneous disorder [5]. Conducting oxides show comparable trends with a debate about the homogeneous character of the charge carrier density or conversely the existence of islands with excess of charge carriers. Recent literature (see *e.g.* discussion in Ref. [10]) focus on the localization of charge carriers in CuO_2 planes in high-T_c oxide superconductors with an incoherent conductivity in the direction perpendicular to the planes. Another aspect of charge carrier localization manifests itself *via* the abundant literature concerning the observation of "stripes" in nickelates [11], manganites [12] or cuprates [13,14].

[a] e-mail: gervais@delphi.phys.univ-tours.fr
[b] UMR 6157 CNRS/CEA

References [5–7] for conducting polymers for example, and references [8–14] among many others for oxide superconductors, thus point towards a non-homogeneous charge carrier density in many systems where the doping level does not rank them as a conductor like a conventional metal. In addition, contrary to metals, the screening is generally incomplete in conducting oxides and in conducting polymers as well, as probed by the signature of polar phonon in infrared reflectivity spectra. The relation of incomplete screening to possible inhomogeneities of charge carrier density is another key question. The conventional Drude model applies to coherent motions of "free electrons" in systems in which screening assumes vanishingly small interaction between charge carriers, expressed for example *via* the Thomas-Fermi wavevector (see *e.g.* Ref. [15]). There are at least two possible important consequences of incomplete screening in a system in which the electronic charge density would be homogeneous: (i) the relevance of a possible polaronic conductivity mechanism, instead of a free electron model for polar media in which the Coulombic field is no longer negligible, (ii) the incomplete Thomas-Fermi exponential decay consequences, such as interactions of charge carriers. Things might be more complicated in inhomogeneous systems.

The electronic transport signatures in conducting materials that show important deviation from conventional metals, therefore, deserve specific consideration in the intermediate carrier density regime. This is particularly important from the perspective of technological applications since it concerns many classes of materials of great interest such as conducting oxide ceramics, films, oxide superconductors, giant magneto-resistance (GMR) materials, and conducting polymers. An example in the case of the latest type of materials is presented here. Within the class of conducting polymers, polyaniline (PANI) is unique in that the electronic structure and electrical properties can be reversibly controlled by both charge transfer doping and protonation [16]. The wide range of associated electrical and optical properties coupled with excellent environmental and thermal stability, make polyaniline attractive as an electronic material for potential use in a variety of technological applications. Recently, progress in the synthesis and processing of the polyaniline protonated with camphor sulfonic acid (PANI-CSA) in metacresol has greatly improved the homogeneity of the material and significantly reduced the degree of structural disorder [17]. These structurally improved materials provide opportunities to study the metal-insulating transition and the intrinsic metallic state focusing on the role of disorder on localization phenomena. The dedoping dependence of the infrared-visible reflectivity of PANI-CSA is reported here and analyzed in terms of optical conductivity both by Kramers-Kronig inversion and attempts to fit with several models of dielectric response.

2 Experimental

The emeraldine base form of the polyaniline was synthesized chemically according to reference [18] by the oxidative polymerization of aniline in an aqueous HCl solution. The mixture of aniline and ammonium persulfate was stirred for 72 hours at −40 °C. The HCl doped polyaniline was then dedoped by submerging the polymer in an ammonic solution. PANI-CSA doped polymer was then prepared by mixing two equivalents of emeraldine base and one equivalent of camphor sulfonic acid. The molar ratio of CSA to phenyl-nitrogen repeat unit was 0.5 for complete protonation of the polyaniline to the emeraldine salt form [19]. High quality films of PANI-CSA were then obtained by casting the material from solution in meta-cresol [19]. Films were deposited onto glass optically flat surfaces and then air-dried for 48 hours at 50 °C. The thickness of the films exceeded several micrometers, thus was larger than the electromagnetic penetration depth to avoid the transmittance of the incident radiation. Samples B and C were dedoped under ammoniac vapor. The DC conductivity of sample A that is nominally doped reached 150 $\Omega^{-1}\,\mathrm{cm}^{-1}$, that of sample B that was dedoped for 10 minutes amounted to 60 $\Omega^{-1}\,\mathrm{cm}^{-1}$, whereas the conductivity of sample C that was dedoped for one hour was found to be lower than 2 $\Omega^{-1}\,\mathrm{cm}^{-1}$. The reflectivity spectrum of the polymer film was measured at room temperature with an IFS 113 Bruker infrared Fourier transform spectrometer in the wavenumber range 25–15,000 cm^{-1}.

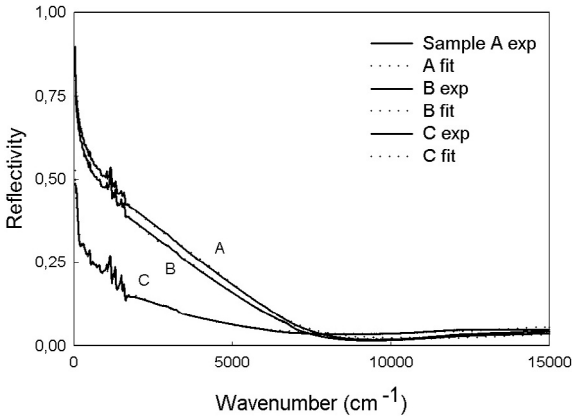

Fig. 1. Experimental reflectivity spectra (dots) for three levels of doping (see text and Tab. 1). Best fit (full lines) of the model equation (13) to reflectivity data.

3 Results and discussion

The reflectivity spectra of PANI-CSA samples are shown in Figure 1 *versus* doping. It is characteristic of a conducting material with a reflectivity that tends towards 100% in the lower energy region. However, even if the reflectivity is maximum at the lowest measured frequency, the reflectivity does not exceed 0.5 at the lowest measured frequency for sample C. The spectra are similar to those reported in reference [20]. In most conducting oxides, the usual Drude model

$$\tilde{\varepsilon} = \varepsilon_\infty \left[1 - \frac{\Omega_p^2}{\omega(\omega - \mathrm{i}\gamma_0)}\right] \qquad (1)$$

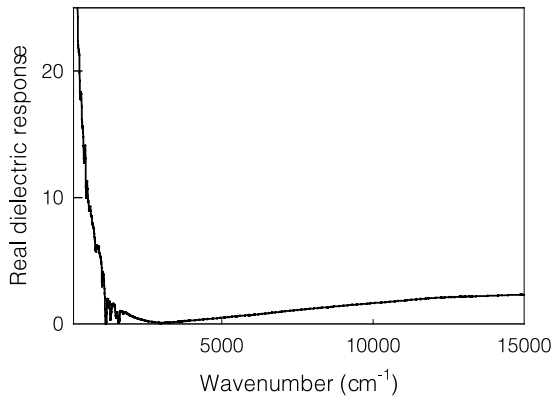

Fig. 2. Wavenumber dependence of the real part of the dielectric constant for the three samples.

is unable to fit the experimental reflectivity. The same was reported in the conducting polymer sample studied in reference [20]. An "extended Drude" model,

$$\tilde{\varepsilon} = \varepsilon' - \mathrm{i}\varepsilon'' = \varepsilon_\infty \left[1 - \frac{{\Omega_p}^2}{\omega[\omega - \Pi(\omega)]}\right] \tag{2}$$

is usually tested in that case, where $\Pi(\omega) = \Delta\omega(\omega) + \mathrm{i}\gamma(\omega)$ represents a self-energy function instead of a constant damping, the imaginary part of which being a plasmon damping function $\gamma(\omega)$, and the real part a renormalization of the plasmon energy. The damping function may be evaluated *via*

$$\gamma(\omega) = \frac{\omega\varepsilon''(\omega)}{\varepsilon_\infty - \varepsilon'(\omega)} \cdot \tag{3}$$

But, since damping cannot assume negative values, the condition $\varepsilon'(\omega) < \varepsilon_\infty$ should be obeyed for any ω. Figure 2 shows that this is not the case in the whole spectral range since the real part of the dielectric constant largely exceeds ε_∞ in the far-infrared for all three samples. Another extension of the Drude model has been tested in PANI-CSA [21]. It is derived from the factorized form of the dielectric function and is based upon the extension of the Lyddane- Sachs-Teller relationship in the form [22,23]

$$\tilde{\varepsilon} = \varepsilon_\infty \prod_j \frac{\Omega_{jLO}^2 - \omega^2 + \mathrm{i}\gamma_{jLO}\omega}{\Omega_{jTO} - \omega^2 + \mathrm{i}\gamma_{jTO}\omega} \tag{4}$$

that expresses that longitudinal optical modes are the complex zeroes of the dielectric response, while the transverse modes are its complex poles. This is a straightforward application of one of the Maxwell relationships. In equation (4), Ω represents the frequencies and γ the damping of each phonon (or other type) oscillator j, respectively, and $\varepsilon_\infty = 1 + \chi_{\mathrm{electronic}}$ is the "high-frequency" dielectric constant from the viewpoint of the infrared spectroscopist. In the presence of mobile charge carriers, the general formula (4) may be complemented in the form [23,24]

$$\tilde{\varepsilon} = \varepsilon_\infty \left[\prod_j \frac{{\Omega_{jLO}}^2 - \omega^2 + \mathrm{i}\gamma_{jLO}\omega}{{\Omega_{jTO}}^2 - \omega^2 + \mathrm{i}\gamma_{jTO}\omega} - \frac{\Omega_P^2 + \mathrm{i}(\gamma_P - \gamma_0)\omega}{\omega(\omega - \mathrm{i}\gamma_0)}\right] \tag{5}$$

that permits the separation of the contribution of charge carrier motion (*i.e.* without restoring force) and of the other excitations (such as phonons, trapped polarons). Ω_P is the screened Drude plasma frequency as in (1) related to the charge carrier density n *via*

$$\Omega_P^2 = \frac{ne^2}{m^*\varepsilon_V\varepsilon_\infty} \cdot \tag{6}$$

γ_P represents the linewidth of the plasma response centered at $\omega = \Omega_P$ and γ_0 is the linewidth of the absorption centered at $\omega = 0$. m^* is the carrier effective mass. The usual Drude model equation (1) is recovered on setting $\gamma_0 = \gamma_P$. The reflectivity is then calculated from the dielectric function *via*

$$R = \left|\left(\sqrt{\tilde{\varepsilon}} - 1\right) / \left(\sqrt{\tilde{\varepsilon}} + 1\right)\right|^2 \tag{7}$$

and the spectral conductivity $\tilde{\sigma}$ *via*

$$\tilde{\varepsilon} = \varepsilon_\infty - \frac{\mathrm{i}\tilde{\sigma}}{\varepsilon_V\omega} \tag{8}$$

where ε_V is the dielectric constant of vacuum. This "double-damping Drude" (DDD) model has been shown to yield a much better fit than the usual Drude model for conducting oxide materials (see a review in Refs. [23] and [24] for example). It was tempting, therefore, to try to apply this model to a conducting polymer, the spectrum of which does not exhibit the usual Drude-type profile. Results of reference [21] showed the success of this method. Similar excellent fits to reflectivity data can be achieved with spectra of samples A, B and C. However, upon examining the phonon oscillator strengths deduced from the fitting parameters *via*

$$\Delta\varepsilon_j = \frac{\varepsilon_\infty}{\Omega_{jTO}^2} \frac{\prod_k (\Omega_{kLO}^2 - \Omega_{jTO}^2)}{\prod_{k\neq j} (\Omega_{kTO}^2 - \Omega_{jTO}^2)} \tag{9}$$

one notes a large variation of the phonon oscillator strengths with doping. The sum of oscillator strengths indeed amounts to 2.6 in sample C, whereas it reaches 3.6 in sample B and 3.8 in sample A. Such a variation compared to the level of the dielectric constant $\varepsilon_\infty = 2.5$ found roughly independent of doping, seems to be physically unrealistic. The oscillator strength, indeed, is related to the Born effective charge carried by the atoms that is related to the electronegativity difference and is, a priori, expected not to vary sensitively with doping.

There is an alternative that was used in several works [4,20]. A localization of carriers by disorder is assumed to decrease the Drude contribution towards low

Table 1. Parameters that yield the best fit to reflectivity data of sample C. All frequencies and dampings are in cm^{-1} units. Others are dimensionless. Broad bands denoted by stars (*), with large damping and large oscillator strengths are not phonons and are assigned to polarons.

Ω_{TO}	γ_{TO}	$\Omega_{\rm LO}$	$\gamma_{\rm LO}$	$\Delta\varepsilon$
238.6	29.7	239	30	0.019
284	60	290.5	69.5	0.19
369.1	29.4	369.5	29.5	0.009
407.2	80	411	79.5	0.075
499.2	49.7	506.5	40.3	0.123
561.3	101	570.6	121	0.11
697	35.2	699.2	34.6	0.024
788.5	80	796.4	80	0.072
1157.8	100	1169.9	44	0.113
1236.9	90	1254.5	70	0.129
1293.2	35	1303.8	35	0.05
1500.9	70	1509.2	45	0.083
1564.2	50	1573.2	50	0.114
1626.4(*)	1500	1871	2000	0.566
2900.9	100	2905	100	0.0054
3200	100	3201.9	100	0.0025
16900(*)	9400	17550	12350	0.175
Ω_P	γ_P	a	b	
600	9000	7	6	
$\varepsilon_\infty = 2.3$				

frequencies in the form

$$\tilde{\sigma}(\omega) = \tilde{\sigma}_D(\omega)\left(1 - \frac{1 - a\sqrt{\omega}}{b}\right) \tag{10}$$

where parameters a and b are related to the carrier relaxation time τ, to the mean free path Λ and to the wave vector q_F at the Fermi level *via*

$$a = \sqrt{3\tau} \tag{11}$$

$$b = (q_F\Lambda)^2. \tag{12}$$

Taking account of the phonons (and other possible oscillators like polarons) *via* equation (4) combined with (10), yields

$$\tilde{\varepsilon}(\omega) = \varepsilon_\infty\left(\prod_j \frac{\Omega_{jLO}^2 - \omega^2 + \mathrm{i}\gamma_{jLO}\omega}{\Omega_{jTO}^2 - \omega^2 + \mathrm{i}\gamma_{jTO}\omega} - \frac{\Omega_P^2}{\omega(\omega - \mathrm{i}\gamma_P)}\left(1 - \frac{1 - a\sqrt{\omega}}{b}\right)\right). \tag{13}$$

The best fits of equation (13) to reflectivity spectra of samples A-C are shown in Figure 1. Within this description, the phonon oscillator strength parameters are found to be much more realistic since their sum is confined between 1.1 and 1.3, *viz.* little dependent on doping. In addition, the phonon oscillator strengths are more consistent with the covalent character of the bonds than the values extending from 2.6 up to 3.8 found with the model equation (5). Detailed phonon parameters are given in Table 1 for sample C where they are less screened and evaluated, therefore, with better accuracy. Note that two additional oscillators, too broad for phonons, have been added to achieve a good fit. They are assigned to polarons by analogy with studies in conducting oxides [25–29]. Table 2 reports mobile charge carrier parameters *versus* doping. The pronounced effect of carrier localization on the reflectivity is illustrated in Figure 3 where the reflectivity calculated with the same parameters that yield the best fit, except $a = 0$ and b tending towards infinity to cancel the effect of the last term in equation (13), is compared to the experiment. The doping dependence of the optical conductivity calculated with equation (13) from the best fits is shown in Figure 4. Although the conductivity profiles are very similar to those obtained *via* Kramers-Kronig inversion (Fig. 5), some discrepancies exit. Since the model fits the reflectivity spectra within experimental error, one should ascribe the discrepancies to the errors made by the Kramers-Kronig transformation when residual dispersion exists at both ends of the spectral data. This is the case here since in conducting systems and contrary to insulators, dispersion is effective down to zero frequency. The samples are not transparent in the visible range, indicating remaining dispersion in this region too. The application of the relationship

$$\int_0^{\omega_c} \sigma(\omega')\mathrm{d}\omega' = \frac{\pi e^2}{2}\frac{N_{\rm eff}(\omega)}{m^*} \tag{14}$$

allows the estimate of $N_{\rm eff}$ upon integrating the optical conductivity up to $\omega_{\rm c} = 1.1$ eV (if one assumes that

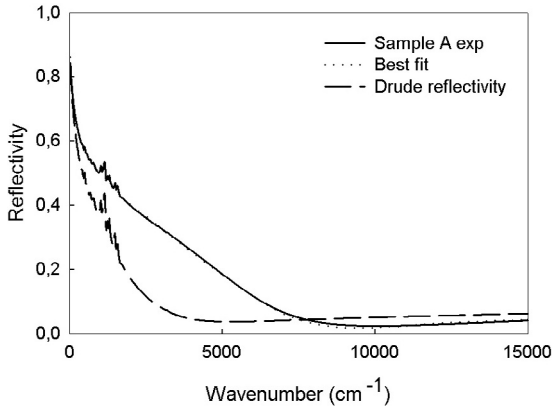

Fig. 3. An example of the effect on the reflectivity of setting $a = 0$ and b tending towards infinity (then assuming normal Drude reflectivity) in the model equation (13), keeping the parameters that yield the best fit to reflectivity data shown in the figure.

Table 2. Plasma frequencies, electronic concentration, carrier relaxation times, and Fermi wavevector times mean free path, deduced from the best fits of the model equation (13) to reflectivity data of samples A-C.

	Sample A	Sample B	Sample C
Ω_P (eV)	0.42	0.36	0.06
$N_{\rm eff}$(1.1 eV) (e/cm^3)	8.4×10^{20}	7.2×10^{20}	2.9×10^{20}
τ (ps)	2.3	2.8	780
$q_F l$	3.3	3.2	2.4

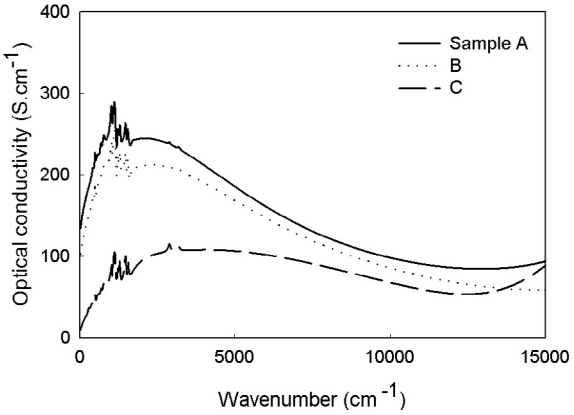

Fig. 4. Doping dependence of the optical conductivity spectra deduced from the best fit of the model equation (13) to reflectivity data.

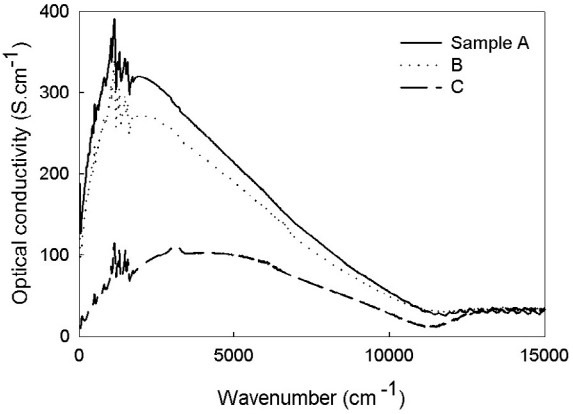

Fig. 5. Doping dependence of the optical conductivity spectra calculated by Kramers-Kronig transformation of reflectivity spectra.

the electron effective mass m^* is the electron mass). Results are given in Table 2. With values ranging from 2.9 to 8.4×10^{20} e/cm^3, we check, therefore, that the electronic density is significantly lower than that of normal metals ($> 10^{22}$ e/cm^3) but is comparable with that ($\sim 10^{21}$ e/cm^3) of high-T_c oxide superconductors.

Do the present results point towards inhomogeneous disorder? In particular, do they support the mechanism of charge transport involving a network of metallic grains connected by resonance tunneling, as proposed recently [30]? The effective electronic density of the most doped sample A, $N_{\rm eff} = 0.84 \times 10^{21}$ cm^{-3}, suggests that this sample might be a good candidate for a test of the model. However, Figures 4 and 5 obtained by two different methods of analysis do not show the expected shape for the spectral conductivity predicted by the model (see Fig. 6 of Ref. [30]). In particular, the spectra do not display an increase of the far-infrared conductivity upon further decreasing frequency after the drop just below the optical phonon frequencies in sample A (nor in other samples either). In addition, the fair agreement of measured DC conductivities with data obtained either from Kramers-Kronig inversion or data fit, does not leave the possibility of an additional transport mechanism that would take place at frequencies below the infrared range. Due to causality relations, the real part of the dielectric response of samples A-C consistently reaches its maximum value at the lowest measured frequency (Fig. 2) instead of becoming negative as expected from the model of reference [30]. We may conclude, therefore, that, even in the most conducting of our samples ($\sigma_{DC} = 150\ \Omega^{-1}\,{\rm cm}^{-1}$), no percolation seems to occur to allow a further increase of the conductivity upon decreasing frequency in the very far infrared as proposed in [30] to explain the results of references [5,31]. Present samples rather suggest homogeneous transport properties.

Small angle neutron scattering studies of (deuterated) PANI-CSA films suggest that the films are heterogeneous and exhibit 30–100 angstroms metallic domains embedded in an insulating matrix [32]. This experimental result supports the interpretation of previous transport studies of conducting polymers in terms of a granular polymeric metal system [33]. Far-infrared absorption of small metallic particles, indeed, was shown to yield very small absorption at low infrared frequency [34], so that one may wonder whether the drop of conductivity upon decreasing frequency could not be understood within another model. Actually, the question is whether samples with DC conductivities as high as 2–150 $\Omega^{-1}\,{\rm cm}^{-1}$, as measured in the present study, could be compatible with a model of small conducting grains separated by insulating domain walls. This is hard to believe since the scope of reference [33] deals with thermally-assisted conductivities much lower than 1 $\Omega^{-1}\,{\rm cm}^{-1}$, well below, therefore, that of samples studied here. Percolation would be needed to accommodate the present high conductivity of sample A, but since no signature of percolation is observed as discussed in the previous paragraph, results rather suggest homogeneous transport properties, at least at length scales less than the electron correlation length.

4 Conclusion

The reflectivity of films of CSA-doped polyaniline with different doping level has been investigated in terms of spectral conductivity, both by Kramers-Kronig transformation and by fitting procedure. Both approaches compare reasonably well. The Drude model in its conventional version is confirmed not to apply to describe these spectra correctly. A general theory of conductivity in media at intermediate charge carrier density, valid for conducting polymers or oxides or other non-metallic conducting media, appears highly desirable. Within this perspective, the parameterization of the conductivity performed here will be useful for comparison of different classes of materials. It appears that the fitting with the double-damping Drude model studied in a previous paper [21] although fitting correctly, implies too large and doping-dependent phonon oscillator strengths, which appears to be physically questionable. We have adapted, therefore, the Anderson

localization model [2] to allow fitting with the factorized form of the dielectric response. Excellent fits have been achieved. The physical parameters that are deduced and their dependence upon doping, appear reasonable. In addition, the method has the merit of discriminating trapped species (polarons) from mobile charge carriers (Drude-like). Further studies *versus* temperature will allow us to complement this approach.

References

1. C.K. Chiang, C.R. Fincher Jr., Y.W. Park, A.J. Heeger, H. Shirakawa, E.J. Louis, S.C. Gau, A.G. MacDiarmid, Phys. Rev. Lett. **39**, 1098 (1977)
2. P.W. Anderson, Phys. Rev. **109**, 1492 (1958)
3. C.O. Yoon, M. Reghu, D. Moses, A.J. Heeger, Phys. Rev. B **49**, 10851 (1994)
4. K. Lee, R. Menon, C.O. Yoon, A.J. Heeger, Phys. Rev. B **52**, 4779 (1995)
5. R.S. Kohlman, J. Joo, Y.G. Min, A.G. MacDiarmid, A.J. Epstein, Phys. Rev. Lett. **77**, 2766 (1996); R.S. Kohlman, A. Zibold, D.B. Tanner, G.G. Ihas, T. Ishiguro, Y.G. Min, A.G. MacDiarmid, A.J. Epstein, Phys. Rev. Lett. **78**, 3915 (1997)
6. J. Joo, S.M. Long, J.P. Pouget, E.D. Oh, A.G. MacDiarmid, A.J. Epstein, Phys. Rev. B **57**, 9567 (1998)
7. A.B. Kaiser, G. Düsberg, S. Roth, Phys. Rev. B **57**, 1418 (1998)
8. X.Q. Yang, D.B. Tanner, M.J. Rice, H.W. Gibson, A. Feldblum, A.J. Epstein, Solid St. Commun. **62**, 335 (1987)
9. Y.H. Kim, A.J. Heeger, Phys. Rev. B **40**, 8393 (1989)
10. D. Munzar, C. Bernhard, T. Holden, A. Golnik, J. Humlicek, M. Cardona, Phys. Rev. B **64**, 24523 (2001)
11. C.H. Chen, S.-W. Cheong, A.S. Cooper, Phys. Rev. Lett. **71**, 2461, (1993)
12. Y. Moritomo, Y. Tomioka, A. Asamitsu, Y. Tokura, Y. Matsui, Phys. Rev. B **51**, 3297 (1995)
13. J.M. Tranquada, B.J. Sternlieb, J.D. Axe, Y. Nakamura, S. Uchida, Letters to Nature **375**, 561 (1995)
14. S. Tajima, T. Noda, H. Eisaki, S Uchida, Phys. Rev. Lett. **86**, 500 (2001)
15. N.W. Ashcroft, N.D. Mermin, *Solid State Physics* (Saunders Company, 1976), Chap. 17
16. W.R. Salaneck, I. Lundstrom, W.S. Huang, A.G. MacDiarmid, Synth. Met. **13**, 291 (1986)
17. G. MacDiarmid, A.J. Epstein, Synth. Met. **65**, 103 (1994)
18. Y. Cao, A.J. Heeger *et al.*, Polymer **30**, 2305 (1989); P. Hourquebie, B. Blondel, S. Dhume, Synt. Metals **85**, 1437 (1997)
19. Y. Cao, G.M. Treacy, P. Smith, A.J. Heeger, Phys. Rev. B **48**, 17685 (1993)
20. K. Lee, A.J. Heeger, Y. Cao, Phys. Rev. B **48**, 14884 (1993)
21. N. Petit, F. Gervais, P. Buvat, P. Hourquebie, P. Topart, Eur. Phys. J. B **12**, 367 (1999)
22. T. Kurosawa, J. Phys. Soc. Jpn **16**, 1298 (1961)
23. F. Gervais, in *Infrared and millimeter waves*, Vol. 8 (Academic Press, 1983)
24. F. Gervais, R.P.S.M. Lobo, Z. Phys. B **104**, 681 (1997)
25. P. Calvani, M. Capizzi, S. Lupi, P. Maselli, A. Paolone, P. Roy, Phys. Rev. B **53**, 2756 (1996)
26. Y. Yagil, E.K.H. Salje, Physica C **256**, 205 (1996)
27. J.P. Falk, A. Levy, M.A. Kastner, R.J. Birgeneau, Phys. Rev. B **48**, 4043 (1993)
28. X.X Bi, P.C. Eklund, J.M. Honig, Phys. Rev. B **48**, 3470 (1993)
29. D.M. Eagles, R.P.S.M. Lobo, F. Gervais, Phys. Rev. B **52**, 6440 (1995)
30. V.N. Prigodin, A.J. Epstein, Synth. Met. **125**, 43 (2002)
31. H.C.F. Matens, J.A. Reedijk, H.B. Brom, D.M. de Leuw, R. Menon, Phys. Rev. B **63**, 73203 (2001)
32. P. Terech, M. Trznadel, P. Rannou, J.P. Travers, M. Nechtshein, J.F. Legrand, D. Djurado, Synth. Met. **101**, 839 (1999)
33. F. Zuo, M. Angelopoulos, A.G. MacDiarmid, A.J. Epstein, Phys. Rev. B **36**, 3475 (1987)
34. D.B. Tanner, A.J. Sievers, R.A. Buhrman, Phys. Rev. B **11**, 1330 (1975)